

**NJC****Synthesis of a deoxyguanosine monophosphate rich propyl methacrylate oligomer**

Journal:	<i>New Journal of Chemistry</i>
Manuscript ID	NJ-ART-02-2018-000989.R1
Article Type:	Paper
Date Submitted by the Author:	13-Apr-2018
Complete List of Authors:	Wilson, Michael; Flinders University, College of Science and Engineering Fenati, Renzo; Flinders University, College of Science and Engineering; University of Melbourne, Amanda Ellis Williams, Elizabeth; CSIRO, Manufacturing Flagship Ellis, Amanda; University of Melbourne, Amanda Ellis; Chemical and Biomedical Engineering

SCHOLARONE™  
Manuscripts

## Synthesis of a deoxyguanosine monophosphate rich propyl methacrylate oligomer

Received 00th January 20xx,  
Accepted 00th January 20xx

DOI: 10.1039/x0xx00000x

www.rsc.org/

Michael J. Wilson<sup>†,§</sup>, Renzo A. Fenati<sup>†,§</sup>, Elizabeth G. L. Williams<sup>‡</sup>, Amanda V. Ellis<sup>§\*</sup>

We report on the first synthesis of a “protected” 5′-dimethoxytrityl-*N*-isobutyryl-2′-deoxyguanosine(dG), 3′-[(2-cyanoethyl)-2-(methacryloyloxy)propyl]-monophosphate monomer through a modified phosphoramidite coupling method. Here, 2-hydroxypropyl methacrylate (HPMA) was coupled to a protected 5′-dimethoxytrityl-*N*-isobutyryl-2′-deoxyguanosine, 3′-[(2-cyanoethyl)-(N,N-diisopropyl)]-phosphoramidite. Subsequent reversible addition fragmentation chain transfer (RAFT) polymerisation of the protected monomer, followed by deprotection, produced poly[2-(deoxyguanosine-3′-phospho)propyl methacrylate] (poly(dG-P-PMA)). In situ <sup>1</sup>H nuclear magnetic resonance spectroscopy showed the polymerisation kinetics were consistent with RAFT with dispersity indices (Đ’s) <1.2. Circular dichroism showed that the isolated deprotected deoxyguanosine rich oligomers formed stacked G-quartets in both Li<sup>+</sup> and K<sup>+</sup> ion solutions. These structures were further investigated with confocal fluorescence microscopy.

### Introduction

The incorporation of nucleic acid derivatives into non-biological systems is an emerging field of polymer science which will enable a diverse new range of applications from DNA printing to biological templating. As an example, natural nucleic acid systems, such as deoxyribose nucleic acid (DNA), exhibit precise sequences with dispersity indices (Đ’s) of effectively 1 through dynamic enzymatic control.<sup>1</sup> Attempts to mimic these systems through synthetic pathways have utilised a number of well-established methods, such as the incorporation of nucleobases and nucleosides (nucleobase + deoxyribose) into existing synthetic polymerisation methods including free radical,<sup>2-5</sup> emulsion<sup>6,7</sup> and condensation<sup>8,9</sup> polymerisations. The resulting polymers have shown the ability to bind selectively and template chain length. To date there have been no reports on the incorporation of nucleoside monophosphates (nucleotides) into polymers a step required to produce synthetic polymers that have the potential to mimic synthetic DNA.

To this end this paper investigated the attachment of deoxyguanosine monophosphate (dG) to methacrylate-based oligomers via reversible addition fragmentation chain transfer (RAFT) polymerisation in an attempt to show that such polymer/nucleotide hybrids could exhibit the specificity of binding afforded to active dG functionalities.

The modification of polymers with dG (Fig. 1a) affords an entirely new opportunity to construct polymeric macromolecular architectures based on guanine-quartets (G-quartets) (Fig. 1b). These G-quartets are stabilised via the binding of 4 guanine units through the Hoogsteen face, normally around a cation, as shown in Fig. 1b. Multiple G-quartets form a macrostructure called a G-quadruplex which are either inter- or intra-molecular assemblies<sup>10</sup> and are typically the most stable of the secondary structures.<sup>11-13</sup> G-quadruplexes have previously found uses in cancer biology<sup>14,15</sup> and novel therapeutics<sup>16,17</sup> through to nanoelectronics<sup>18</sup> and nanomechanical systems.<sup>19</sup> Their addition into a synthetic polymer based system gives a unique macromolecular structure for a range of biological applications.

In this work a “protected” 5′-dimethoxytrityl-*N*-isobutyryl-2′-deoxyguanosine (dG), 3′-[(2-cyanoethyl)-2-(methacryloyloxy)propyl]-monophosphate monomer was first synthesised by modifying a traditional phosphoramidite coupling method.<sup>20-22</sup> Gram quantities of the monomer were produced and polymerised using RAFT polymerisation.

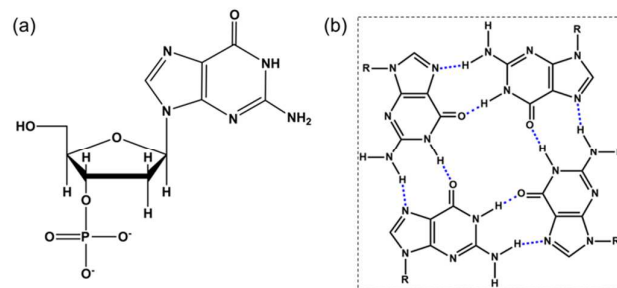


Fig. 1 Schematic of (a) the deoxyguanosine monophosphate (dG) and (b) binding structure of a G-quartet around a cation.

<sup>†</sup> Flinders Centre for Nanoscale Science and Technology, Flinders University, Bedford Park, South Australia, 5042, Australia.

<sup>‡</sup> CSIRO Manufacturing Flagship, Private Bag 10, Clayton, Victoria, 3168, Australia.

<sup>§</sup> School of Chemical and Biomedical Engineering, University of Melbourne, Grattan Street, Victoria 3010, Australia; Amanda.ellis@unimelb.edu.au

After RAFT polymerisation, the oligomer/protected nucleotide hybrid was then deprotected and detritylated, resulting in an oligomer with free dG's.

The functionality of this hybrid material was then tested with aqueous lithium and potassium ion solutions to show feasibility of G-quartet formation and the resulting structures were analysed using circular dichroism, UV-visible spectrophotometry, fluorescence and confocal microscopy.

## Experimental

### Reagents

Powdered 4,5-dicyanoimidazole (DCI) was obtained from GlenTech, USA. 5'-dimethoxytrityl-*N*-isobutyryl-2'-deoxyguanosine, 3'-[(2-cyanoethyl)-(*N,N*-diisopropyl)]-phosphoramidite (denoted DMT-dG-CE phosphoramidite, Scheme 1 (1), Table S1) was obtained from Link Tech, UK. 2-hydroxypropyl methacrylate (HPMA), 4-cyano-4-(phenylcarbonothioylthio)pentanoic acid *N*-succinimidyl ester (RAFT agent), lithium acetate (LiAc), potassium acetate, ethyl acetate (EtAc), dichloromethane (DCM), triethylamine (TEA), dimethylacetamide (DMAC), tetrahydrofuran (THF), dimethylsulfoxide (DMSO) and all other solvents (including deuterated solvents for NMR) were obtained from Sigma-Aldrich, Australia. The cationic dye, ATTO 550 was purchased from ATTO-TEC GmbH, Germany. Azobisisobutyronitrile (AIBN) was obtained from Sigma Aldrich, Australia and recrystallised from methanol before use. All other reagents were used as received.

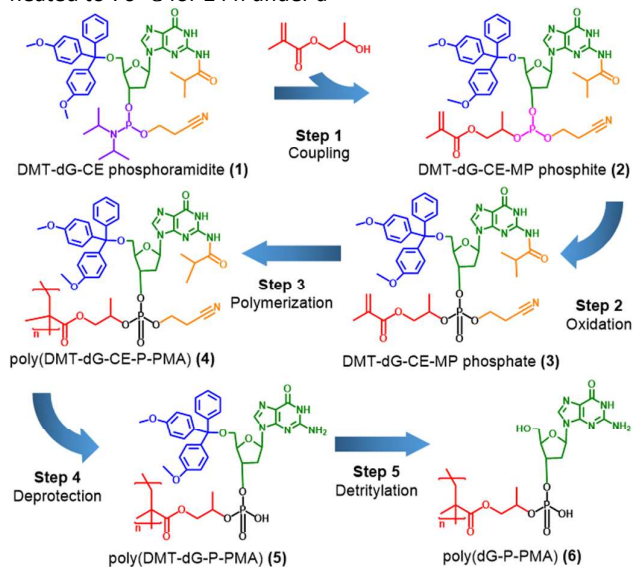
### Synthesis of 5'-dimethoxytrityl-*N*-isobutyryl-2'-deoxyguanosine, 3'-[(2-cyanoethyl)-2-(methacryloyloxy)propyl]-monophosphate (3)

HPMA (0.2 M) and DCI (0.8 M) solutions were prepared with dry acetonitrile and stored over 3 Å molecular sieves under a N<sub>2</sub> atmosphere. Each solution (6 mL) was added to DMT-dG-CE phosphoramidite (1) (1 g) in the vial as supplied and sonicated for 1 min before being cooled to 4 °C for 4 h. The reaction was then quenched with 45:45:10 EtAc:DCM:TEA (v/v, 4 mL) and left for 12 h at 0 °C. The resulting mixture containing 5'-dimethoxytrityl-*N*-isobutyryl-2'-deoxyguanosine, 3'-[(2-cyanoethyl)-2-(methacryloyloxy)propyl]-monophosphite (denoted DMT-dG-CE-MP phosphite, Scheme 1 (2), Table S1) was then phase extracted from water into DCM and oxidised via evaporation at ambient temperature under compressed air. The yield was recorded as 0.82 g (76%). The product was denoted DMT-dG-CE-MP phosphate (Scheme 1 (2), Table S1).

### Synthesis of poly-5'-dimethoxytrityl-*N*-isobutyryl-2'-deoxyguanosine, 3'-[(2-cyanoethyl)-(2-propyl methacrylate)]-phosphate (4)

The DMT-dG-CE-MP phosphate monomer (3) (1.54 g, 75 mg/mL) was combined with the RAFT agent and AIBN at a molar ratio of 20:4:1 in dry acetonitrile. The molar ratio of 20:4:1 was designed to yield oligomers for easier characterisation and solubility studies. The solution was then degassed using dry N<sub>2</sub> for 45 min, typically resulting in a

decrease in solvent volume of between 5-15 %v/v, and then heated to 70 °C for 24 h under a



**Scheme 1.** Proposed coupling of HPMA to protected DMT-dG-CE phosphoramidite (1) and subsequent polymerisation, deprotection and detritylation to form poly[2-(deoxyguanosine-3'-phospho)propyl methacrylate] (poly(dG-P-PMA) (6)). The colour indicates the substituents and their incorporation into the nomenclature; the deoxyribonucleoside (green), 3'-dimethoxytrityl protecting group (DMT, blue), isobutryl and cyanoethyl protecting groups (CE, orange), and phosphoramidite with diisopropylamine protecting group (purple). Addition of the HPMA (red) converts the phosphoramidite into a phosphite (pink). Subsequent oxidation results in a phosphate (black).

sealed N<sub>2</sub> atmosphere. Following thermal quenching the oligomer was isolated by precipitation. The product was denoted poly(DMT-dG-CE-P-PMA) (Scheme 1 (4), Table S1).

### Deprotection of poly(DMT-dG-CE-P-PMA) (4)

The crude poly(DMT-dG-CE-P-PMA) (4) (0.8 g) was placed in a round bottom flask with 30% ammonia in water (50 mL). The solution was heated to 50 °C for up to 24 h until the sample dissolved and the solution turned clear. Subsequently, the solution was filtered, and the eluent dried under N<sub>2</sub>. The product was denoted poly(DMT-dG-P-PMA) (5).

### Detritylation of poly(DMT-dG-P-PMA) (5)

Poly(DMT-dG-P-PMA) (5) (0.4 g) was placed into 80% acetic acid in water (10 mL) for 20 min producing a bright orange colour. Lithium acetate (1.5 M, 1 mL) was then added until the orange colour was removed. The solution was cooled to 0 °C for 30 min, then 100 µL of the solution was centrifuged to isolate the final oligomeric product poly[2-(deoxyguanosine-3'-phospho)propyl methacrylate] (Scheme 1 (6), Table S1). The solid white product was denoted poly(dG-P-PMA) (6).

### Characterisation

**Solubility of poly(dG-P-PMA) (6).** The solubility of the final deprotected, detritylated oligomer (6) was evaluated in DMAC, chloroform, THF and water:isopropanol mixtures. This was

determined qualitatively by adding 10 mg of the poly(dG-P-PMA) (**6**) oligomer to 1 mL of solvent with sonication for 10 min. The polymer showed no dissolution in either DMAC, chloroform or THF. Water formed a stable colloidal suspension. The opacity of the solution increased with increasing ratio of isopropanol and at 100% isopropanol resulted in a completely transparent solution. Poly(dG-P-PMA) (**6**) showed moderate solubility in DMSO and so this was used for NMR studies of the final product.

**<sup>1</sup>H Nuclear magnetic resonance (NMR) spectroscopy.** Structural NMR spectra of the DMT-dG-CE-MP phosphate (**3**) were measured on a Bruker 600 MHz spectrometer in deuterated chloroform using a 5 mm inverse multinuclear probe for <sup>31</sup>P and a 5 mm triple resonance (HCN) probe for <sup>1</sup>H. Structural NMR spectra of the poly(dG-P-PMA) (**6**) were measured on a Bruker 600 MHz spectrometer in deuterated DMSO using a 5 mm triple resonance (HCN) probe for <sup>1</sup>H. To determine the polymerisation kinetics in-situ NMR polymerisation measurements were conducted on a Bruker 400 MHz spectrometer using a 5 mm inverse multinuclear probe measuring <sup>1</sup>H. The NMR was preheated to 70 °C prior to inserting the NMR tube. A degassed solution of DMT-dG-CE-MP phosphate (**3**) (1 mL, 75 mg/mL) with RAFT agent and AIBN at a molar ratio of 20:4:1 in d3-acetonitrile was sealed in a glass NMR tube under an N<sub>2</sub> atmosphere. The NMR tube was then inserted into the instrument and measurements were taken for 2.5 min at 10 min intervals for a total cycle time of 12.5 min and repeated for 850 min. The integration ratio of the monomer peak at  $\delta = 5.6$  ppm was compared to the peak associated with trace TEA at  $\delta = 3.1$  ppm to determine conversion.

**Electron spray ionisation mass spectrometry (ESI-MS).** The ESI-MS spectrum was recorded on a Waters Synapt HDMS (Waters, Manchester, UK) in electrospray positive ion mode, using an infusion of 0.05 mM sodium formate solution for calibration.

**Size-exclusion chromatography (SEC).** The average molecular weight (M<sub>n</sub>) and Đ of poly(DMT-dG-CE-P-PMA) (**4**) synthesised via the large-scale process was determined using SEC on a Waters 2690 Separation Module using a Waters 410 differential refractometer. Two Agilent PLgel 5  $\mu$ m MiniMIX-C columns were used in series with an Agilent guard column. The eluent was HPLC grade tetrahydrofuran. Calibration was conducted using polystyrene standards.

**UV-visible spectroscopy.** Samples were prepared by re-suspending the final product, poly(dG-P-PMA) (**6**), (after centrifugation described previously) in water:isopropanol 10:1 (v/v) (1 mL) with mild sonication. Multiple solutions were prepared for each instrument analysis. For experiments where (**6**) was doped with potassium acetate this was performed by taking 300  $\mu$ L of the above solution and adding in 3  $\mu$ L of aqueous potassium acetate (2.5 M). This results in a doping of 25 mM of potassium acetate. UV-Visible spectra were obtained on the NanoDrop 1000 micro-volume spectrophotometer. 1.5  $\mu$ L sample volumes were measured with 0.2 mm path length and 3 nm resolution.

**Circular dichroism (CD).** CD spectra of 300  $\mu$ L each of poly(HPMA), poly(dG-P-PMA) (**6**) as isolated with lithium acetate and poly(dG-P-PMA) (**6**) doped with potassium acetate (25 mM) were recorded on an Aviv Biomedical Model 410 (USA) equipped with Peltier-controlled thermostat housing unit using a SQ-grade cuvette, with a path length of 1 mm. Spectra were obtained at 25 °C using a scanning rate of 15 nm min<sup>-1</sup>, bandwidth of 1 nm, 1 nm interval data sampling, and a single accumulation. Circular dichroism annealing data was obtained at the 261 nm wavelength with a 1 nm slit and 5 °C per min and equilibrated for 30 s before recording measurements for 1 min.

**Fluorescence measurements.** For poly(dG-P-PMA) (**6**) analysis as isolated with lithium acetate, 1x ATTO 550 dye (1  $\mu$ L) was added to 100  $\mu$ L of (**6**) in water:isopropanol 10:1 (v/v) a solution. Then 25  $\mu$ L was transferred into 4 separate plastic vials for analysis. For the poly(dG-P-PMA) (**6**) doped with potassium acetate (25 mM), 1x ATTO 550 dye (1  $\mu$ L) was added to 100  $\mu$ L of the potassium acetate doped solution. Then 25  $\mu$ L was transferred into 4 separate plastic vials for analysis. Fluorescence versus temperature measurements were then conducted on each 25  $\mu$ L sample simultaneously in a Rotor-Gene real-time polymerase chain reaction (PCR) thermocycler using a yellow channel (530  $\pm$  5 nm excitation, 557  $\pm$  5 nm detection) for detection. The samples were heated at 1 °C per min from 30 °C to 95 °C. The fluorescence of each of the 4 solutions of each sample were averaged.

**Confocal laser scanning microscopy (CLSM).** For the poly(dG-P-PMA) (**6**) analysis as isolated with lithium acetate, 1x ATTO 550 dye (1  $\mu$ L) was added to 100  $\mu$ L of (**6**) in water:isopropanol 10:1 (v/v) a solution. For (**6**) doped with potassium acetate (25 mM), 1x ATTO 550 dye (1  $\mu$ L) was added to 100  $\mu$ L of the potassium acetate doped solution. Confocal fluorescence microscope images were taken on a Nikon A1R with a 150  $\mu$ m glass cover slide using a 488 nm excitation at 200x magnification and red band detection. Each sample was drop cast onto the glass cover slide and the sample imaged near the glass-solvent interface.

## Results and discussion

### Synthesis of DMT-dG-CE-MP phosphate (**3**)

The DMT-dG-CE phosphoramidite has its active sites orthogonally protected so that subsequent sequential deprotection results in the desired final product.

For this, 5'-dimethoxytrityl-*N*-isobutryl-2'-deoxyguanosine, 3'-[(2-cyanoethyl)-(*N,N*-diisopropyl)]-phosphoramidite (hereafter referred to as DMT-dG-CE phosphoramidite) (Scheme 1 (**1**)) was coupled to 2-hydroxypropyl methacrylate (HPMA).

The DMT-dG-CE phosphoramidite (Scheme 1 (**1**), step 1) was first activated with DCI to remove the diisopropylamine group from the phosphoramidite group (Scheme 1, purple) and generate the activated intermediate. DCI was used instead of the commonly used tetrazole<sup>20</sup> as it was in line with DCI's improved efficiency when working with smaller substituents.<sup>23</sup> DCI's enhanced nucleophilicity with lower acidity helps to

ensure the retention of the isobutryl protecting group on the guanine nucleobase (Scheme 1, orange) and reduces phosphorylation during synthesis. The addition of DCI created an unstable intermediate which then reacted with the secondary alcohol of HPMA after its addition (Scheme 1, red). One molar equivalent of HPMA in dry acetonitrile was then added to the activated DMT-dG-CE phosphoramidite (**1**) mixture. This resulted in the “protected” DMT-dG-CE-MP phosphite (**2**) in gram quantities at >75% yield. The reaction was then quenched with a 45:45:10 EtAc:DCM:TEA (v/v) solution. This effectively deactivated any DCI remaining in the solution.

In order to complete the formation of the phosphate (P(V)) from phosphite (P(III)) (Scheme 1, Step 2) the DCM phase extract was oxidised with compressed air under controlled conditions (Scheme 1, Step 3). DCM phase extraction, isolated the DMT-dG-CE-MP phosphite (**2**) and a small amount of DMT-dG-CE-MP phosphate (**3**). The work-up removed any unreacted HPMA and any water soluble protonated monophosphate that did not couple to the HPMA. Compressed air was used for the oxidation rather than the typically used I<sub>2</sub> treatment<sup>20-22</sup> this is because when undertaking the subsequent RAFT polymerisation of (**3**) halide addition to the vinyl moiety must be avoided. Furthermore, trace iodine in the resulting product would require a more intensive workup to prevent a competitive halide mediated polymerisation. Alternative oxidants were considered but these either posed a similar problem, or were a peroxide that may have acted as a radical initiator.<sup>10,24</sup>

ESI-MS of the DCM phase extract confirmed the monomer coupling (Scheme 1, Step 1) (Fig. 2). The theoretical mass of (**1**) was 839 m/z. The mass for (**2**) was 883 m/z and its sodium adduct was 905 m/z. An additional minor peak at 921 m/z was observed due to (**3**), showing moderate oxidation of the phosphite.

Support for HPMA coupling to (**1**) was shown in the solution <sup>1</sup>H nuclear magnetic resonance (NMR) analysis. Fig. 3a shows the <sup>1</sup>H NMR spectra of (i) (**1**) and (ii) (**3**). Fig. 3a(i, a) shows the diisopropylamine group ((CH<sub>3</sub>)<sub>2</sub>CH-N, multiplet, δ = 2.9 ppm) on (**1**). This peak was notably absent in (**3**) (Fig. 3a(ii)). The newly attached propyl methacrylate moiety on (**3**) was observed as two vinyl peaks at approximately δ = 6.1 ppm (Fig. 3a(ii, b) and δ = 5.6 (Fig. 3a(ii, c).

A CH<sub>2</sub> adjacent to acrylate at δ = 4.2 (Fig. 3a(ii, d) and a CH<sub>3</sub> adjacent to the vinyl peak at δ = 1.4 (Fig. 3a(ii, e) ppm was also

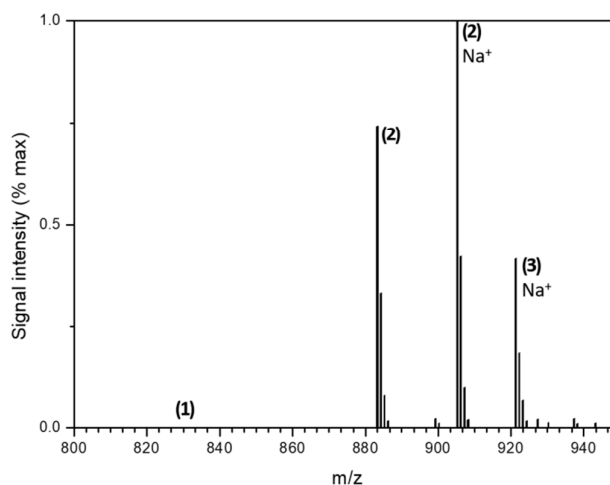
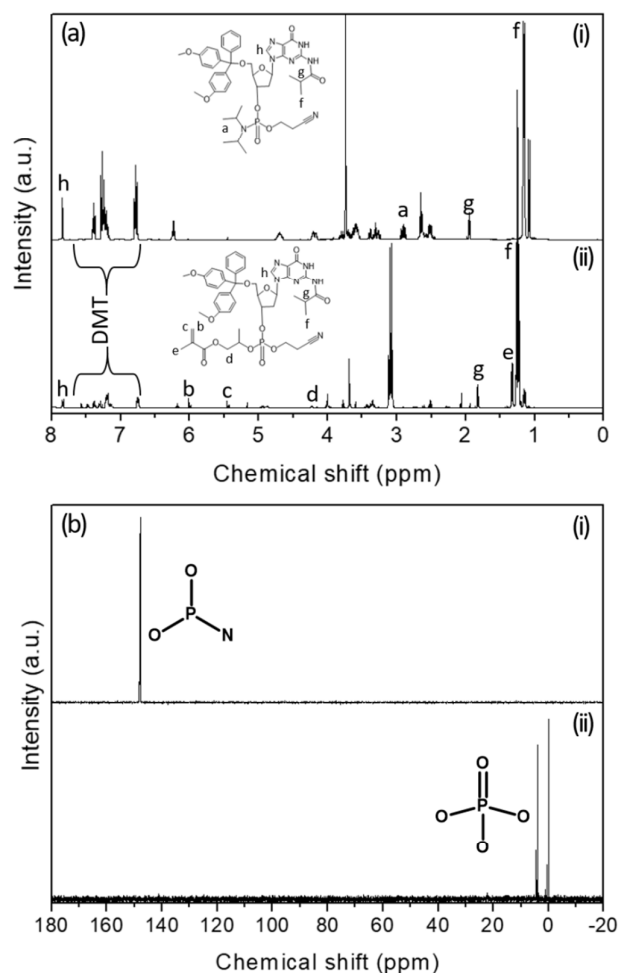


Fig. 2 ESI-MS spectrum of the crude DMT-dG-CE-MP phosphite (**2**), the sodium adduct, and some formation of the DMT-dG-CE-MP phosphate (**3**). Note the lack of peak attributed to the uncoupled phosphoramidite (**1**).

observed in the spectrum of (**3**) with all peaks at the expected integration, confirming HPMA coupling. Confirmation of the phosphorous oxidation from (**1**) to (**3**) was achieved using solution <sup>31</sup>P NMR spectroscopy, in deuterated chloroform. A peak shift from δ = 148 ppm, associated with the P(III) oxidation state of (**1**) (Fig. 3b(i)), to a pair of split peaks at δ = 0 ppm and δ = 4 ppm peaks centred around δ = 2 ppm, associated with the P(V) oxidation state of the (**3**) (Fig. 3b(ii) and inset for expanded region)), was observed.<sup>25</sup> This pair of peaks were due to the two isomeric forms of the [2-(methacryloyloxy)propyl] group on (**3**). The <sup>3</sup>J<sub>PH</sub> coupling of these isomeric forms was 20 Hz. This is an important step as it shows that the phosphate has formed and it is this that gives added functionality to the polymer/nucleotide hybrid. The oxidation from P(III) to P(V) is an important step as this prevents the formation of polyphosphates when the monomer is polymerised under RAFT conditions in the preceding step.



**Fig. 3** (a) <sup>1</sup>H NMR spectra of (i) DMT-dG-CE phosphite (**1**) and (ii) DMT-dG-CE-MP phosphate monomer (**3**) showing the peak allocation, note the 6.7-8 ppm region with peaks attributed to the DMT protons, and (b) <sup>31</sup>P NMR spectra of (i) DMT-dG-CE phosphoramidite (**1**) and (ii) DMT-dG-CE-MP phosphate monomer (**3**). The inset is an expanded region from -1 to 6 ppm. Run at 400 MHz in d<sub>3</sub>-acetonitrile.

It also implies that the hybrid will now have the negative charge attributed to typical DNA constructs.

#### RAFT polymerisation of poly(DMT-dG-CE-P-PMA) (**4**)

After confirmation of the synthesis of the monomer (**3**), it was then used for RAFT polymerisation using 4-cyano-4-(phenylcarbonothioylthio)pentanoic acid *N*-succinimidyl ester as the chain transfer agent (CTA) and AIBN as the initiator. The reagent ratio was 20:4:1 for the monomer:CTA:initiator. This monomer ratio gave a clear determination of the kinetics for the addition reaction without being altered by secondary effects such as steric hindrance or precipitation at increasing molecular weights.<sup>26</sup>

The CTA chosen was a *N*-hydroxysuccinimide (NHS) protected variant of 4-cyano-4-(phenylcarbonothioylthio)pentanoic acid. This was chosen to prevent both the removal of the 5' DMT protecting group and the subsequent condensation polymerisation with the phosphate moiety under the radical polymerisation conditions.

Any condensation polymerisation within the system would lead to a polyphosphate backbone rather than the desired polyvinyl.

Following subsequent ammonia work will cause hydrolysis of the RAFT agent NHS group leaving a pentanoic acid terminal group on the polymer chain.

Solution <sup>1</sup>H NMR spectroscopy in d<sub>3</sub>-acetonitrile confirmed the formation of the poly(DMT-dG-CE-P-PMA (**4**) oligomer (Fig. 4(i)). Polymerisation was observed as the disappearance of the vinyl peak at  $\delta = 5.6$  ppm (observed in the monomer (Fig. 3a(ii)) and the appearance of a broad shoulder at approximately  $\delta = 1$  ppm from the ethylene polymer backbone (Fig 4(i), a). The peak associated with the C8 proton at  $\delta = 7.8$  ppm (Fig. 4(i), b) and the small broad peak at approximately  $\delta = 5.1$  ppm from the protons on the C2' carbon of the ribose unit (Fig. 4(i), c) confirmed that the protected guanosine functionality had been maintained under the RAFT polymerisation conditions.<sup>27</sup>

The final deprotected and detritylated poly(dG-P-PMA) oligomer (**6**) was measured using <sup>1</sup>H NMR in d<sub>6</sub>-DMSO, Fig. 4(ii). Due to the low solubility of the oligomer the spectrum showed high signal-to-noise. However, it can be noted that the spectrum is simpler compared to Fig. 4(i) suggesting that the polymer is now had bulky moieties removed via deprotection and detritylation. With the detritylation and removal of the aromatic DMT groups the methacrylic backbone peaks are now up-shifted compared to the protected polymer. The methyl peak is observed at approximately  $\delta = 0.4$  ppm and the two ethylene protons are now observed at approximately  $\delta = 0.6$  ppm (Fig. 4(ii), d and e, respectively). The propyl linkage between the phosphate and the methacrylic backbone approximately  $\delta = 1.7$  ppm (Fig. 4(ii), f).

The fully deprotected and detritylated guanosine units is observed as the appearance of peaks from the ribose and guanine. For the ribose, peaks are observed at  $\delta = 5.2$  ppm (C5'-OH) and  $\delta = 5.4$  ppm (H-2') (Fig. 4(ii), g and h, respectively). Finally, for guanine peaks are observed at  $\delta = 6.7$  ppm (NH<sub>2</sub>),  $\delta = 9.6$  ppm (H-8) and  $\delta = 11.5$  ppm (NH) (Fig. 4(ii), i, j and k, respectively). These results confirm the presence of the

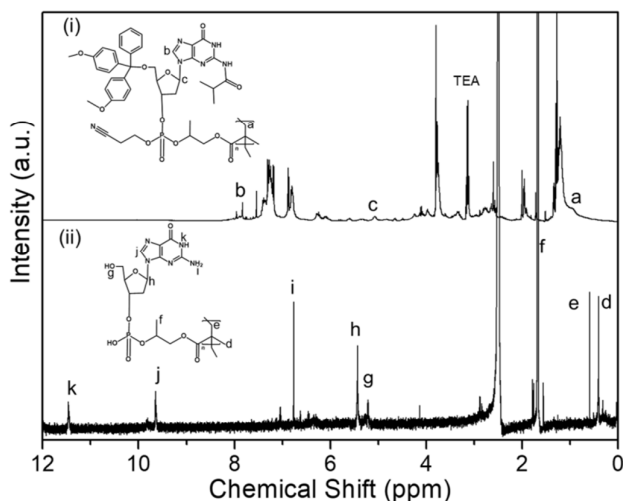


**Fig. 4** Solution  $^1\text{H}$  NMR spectra of (i) poly(DMT-dG-CE-P-PMA) (**4**) at 400 MHz in deuterated acetonitrile with TEA used as an internal standard for kinetic measurements and (ii) poly(dG-P-PMA) (**6**) at 600 MHz in deuterated DMSO. RAFT agent is omitted from inset structures.

guanosine monophosphate nucleotides on the propyl methacrylate backbone.

The kinetics of the polymerisation were monitored using in situ  $^1\text{H}$  NMR spectroscopy (Fig. 5). The monomer (**3**), with CTA and AIBN, were sealed in an NMR tube under  $\text{N}_2$ , then heated to  $70^\circ\text{C}$  in the NMR instrument. Measurements began after a 10 min period and proceeded every 12.5 min for 873 min. Typically for conversion measurements, the disappearance of the vinyl peak at  $\delta = 5.6$  ppm relative to the growing alkyl chain backbone at  $\delta = 1.6$  ppm would be measured.

However, in our case the guanine moieties on the monomer interfered with the alkyl peak at  $\delta = 1.6$  ppm making analysis of conversion using this method impractical. Consequently, the vinyl peak ( $\delta = 5.6$  ppm) was compared to the ethyl proton peak at  $\delta = 3.1$  ppm associated with residual TEA from Step 1 (Fig. 4(i), TEA). TEA acts as an internal standard where the data is normalised relative to the starting TEA/vinyl ratio and the ratio monitored with time

The polymerisation results, with standard deviation over triplicate runs (Fig. 5), showed a short radical initiation period over the first 200 min before the reaction proceeded approximating first order kinetics. The polymerisation gave a 40% conversion between 10-11 h.

SEC of (**4**) in tetrahydrofuran gave a  $M_n$  of approximately 5 kDa with a  $\bar{D}$  of 1.19 after 24 h polymerisation (Fig. S1).

In order for the polymer to have active nucleotide functionalities, polymer (**4**) required deprotection and detritylation (i.e., removal of the cyanoethyl, isobutyl and dimethoxytrityl moieties). This first required the removal of the isobutryl (on the guanine C2 amine) and the cyanoethyl (on the phosphate) protecting groups (Scheme 1, Step 4, orange) from (**4**). Conditions for this deprotection required an excess of ammonia under a sealed atmosphere for 24 h at  $50^\circ\text{C}$ .

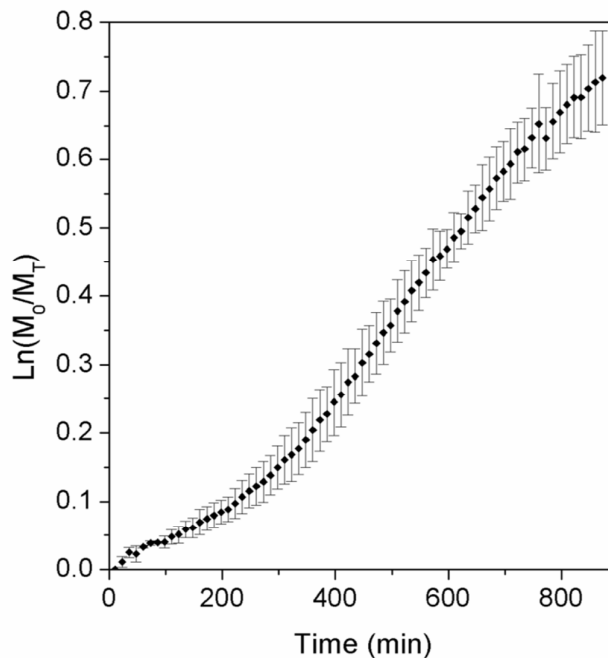


**Fig. 5** Kinetics of the monomer (**3**) via RAFT polymerisation (triplicates) to give (**4**), using in situ  $^1\text{H}$  NMR analysis. Conversion was calculated from the decrease in the vinyl proton ( $\delta = 5.6$  ppm) of (**3**) relative to the ethyl proton ( $\delta = 3.1$  ppm) on the internal TEA standard.

This converted (**4**) to poly(DMT-dG-P-PMA) (**5**) (Scheme 1, Step 4). Any resulting insoluble by-products were removed via filtration. Removal of the dimethoxytrityl protecting group (Scheme 1, blue) was achieved using an excess of acetic acid (Scheme 1, Step 5). To neutralise, aqueous lithium acetate (1.5 M) was titrated with the solution until the orange colour of the free dimethoxytrityl groups disappeared. Subsequently, a white colloidal solution resulted containing the final deprotected and detritylated poly(dG-P-PMA) (**6**). The colloidal solution was then centrifuged at 14000 rpm for 1 min and the supernatant removed. The solid was then resuspended in deionised water:isopropanol (10:1 v/v).

The oligomer (**6**) was then analysed using CD to investigate active deoxyguanosine functionality. CD was used to confirm the presence of stacked G-quartets in oligomer (**6**) isolated with lithium acetate and when subsequently doped with  $\text{K}^+$  ions (25 mM) (Fig. 6a(i)  $\text{Li}^+$  ions (solid line) and  $\text{K}^+$  ions (dashed line)).

Guanine nucleobases, relative to the deoxyribose, exist as either *syn*- and/or *anti*- conformations within a G-quartet (Fig. 6a). By using CD characteristic signals in the CD spectrum enables identification of the various *syn*- and *anti*- conformations of the inter-G-quartet stacking.<sup>19</sup>

A peak at 261 nm is observed in both, consistent with the formation of *anti-anti* stacked G-quartets.<sup>11,19</sup> As these oligomers do not contain a sugar-phosphate backbone, typical of nucleic acids, the directionality cannot be defined as being either parallel or antiparallel. It should also be noted that upon the addition of  $\text{K}^+$  ions there was an increase in the intensity of the peak at 261 nm (Fig. 6b(i) dashed line). This is a result of

increased numbers of G-quartet stacking brought about by the increase in stability that  $K^+$  ions impose on the system.<sup>19</sup>

Both oligomer samples show a large peak at 326 nm (Fig. 6b). This can be attributed to the propyl methacrylate backbone. Here, CD results from the repeating chiral units and the formation of sterically locked nucleotides around the alkyl-backbone. This peak was not observed in the CD spectrum of the pristine poly(HPMA) (Fig. S2(a)) and suggests that the alkyl backbone is locked into a particular orientation arising from the G-quartet stacking, inducing a Cotton effect. Interestingly, this peak does not increase upon the addition of  $K^+$  ions indicating that the rigid structural orientation of the oligomer backbone formed with  $Li^+$  remains even after  $K^+$  ion addition.

Kujawa et al.<sup>28</sup> and Bischofberger et al.<sup>29</sup> have used the change in fluorescence of various compounds to detect the hydrophobic nanodomains in poly(N-isopropylacrylamide) as they formed at elevated temperatures. In this paper ATTO 550 dye was used due to its high quantum yield. Similar ATTO and Alexa dyes have been shown to quench as a result of complexation to other aromatic systems.<sup>30,31</sup> Here, it is shown that the  $\pi$ - $\pi$  complexation, or confinement, of the ATTO 550 dye within the G-quadruplex causes a decrease in fluorescence.

Fig. 6c, right, shows the fluorescence data versus temperature for the oligomer (**6**) stained with ATTO 550 for both the  $Li^+$  (solid squares) and  $K^+$  (open squares) doped oligomer (**6**). For both, fluorescence is shown to increase with temperature. The onset of the fluorescence is approximately 45 °C and 40 °C for  $Li^+$  and  $K^+$ , respectively. This difference remains until both curves plateau at approximately 70 °C. This increase in fluorescence indicated that the particles, shown in Fig. 7, undergo a melting event causing the dye to change in complexation. Similar behaviour was also seen in DNA based G-quadruplexes, Fig S3.

Comparing this to Fig. 6c, left, shows the corresponding change in ellipticity of the 261 nm peak (Fig. 6b(i)) versus temperature for  $Li^+$  (solid line) and  $K^+$  (dotted line) doped oligomer (**6**). When  $K^+$  ions were added to the system there is a corresponding rapid decrease in the 261 nm peak with temperature (Fig. 6c, dotted line), which goes below 0 deg.cm<sup>2</sup> indicating the formation of syn-syn stacked G-quartets, as shown by Tóthová et al.<sup>19</sup> This was not observed for (**6**) isolated with lithium acetate (Fig. 6c, solid line).

Thus, only the addition of  $K^+$  ions results in a change in conformation of the G-quartets with heating. Both showed disruption of structure at higher temperatures, namely 75 °C for  $Li^+$  and 60 °C for  $K^+$  ions. Above these temperatures the guanine Hoogsteen bonding is broken, followed by a conformational change in the alkyl backbone. This rearrangement results in the entire system being annealed and unable to reform the original structure upon cooling. Similar behaviour has been observed previously with nucleobase modified polymers.<sup>32</sup>

CLSM was then used to investigate the ATTO 550 stained oligomer (**6**) in solution with and without  $K^+$  ions (Fig. 7). Fig. 7, left, shows the optical images and the right, the corresponding fluorescence images for poly(HPMA), (**6**) isolated with lithium

acetate and with added  $K^+$  ions (25 mM), respectively. No microparticles were observed for the poly(HPMA), with a uniform distribution of fluorescence observed (Fig. 7a and b).

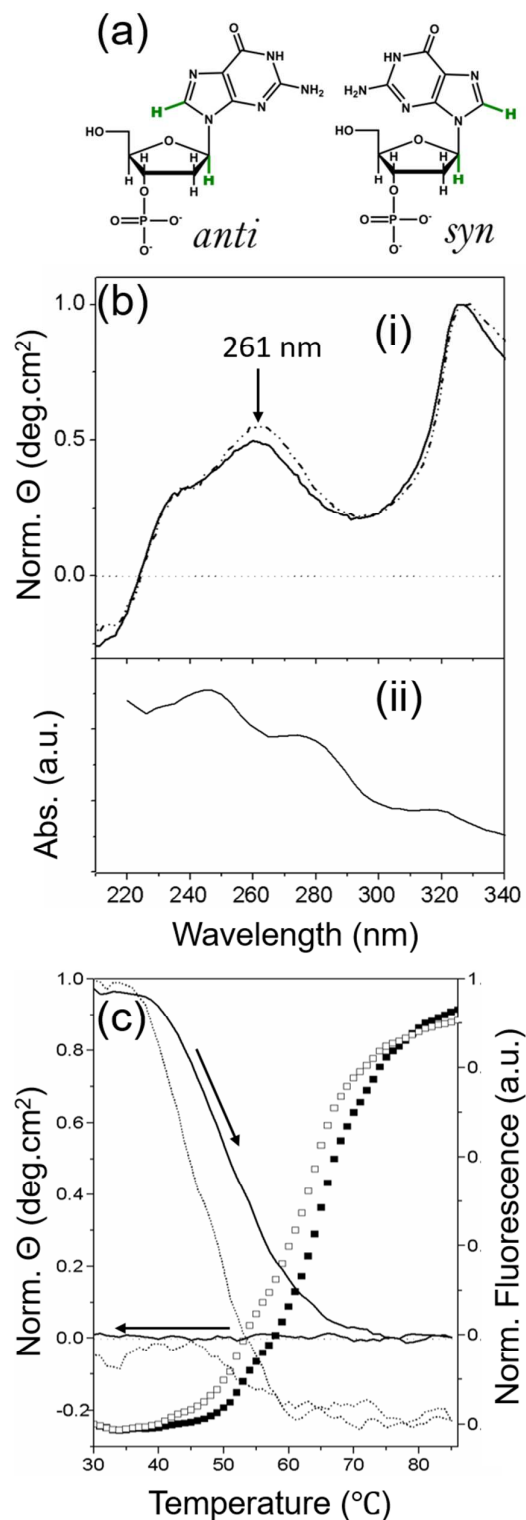




**Fig. 6** (a) *Syn*- and *anti*-conformations of dG based on the location of the protons highlighted in green. (b)(i) CD spectra of poly(dG-P-PMA) (**6**) in 10:1 (v/v) water:isopropanol with (i) Li<sup>+</sup> (solid line) and added K<sup>+</sup> (dashed line) cations (25 mM) normalized to the 326 nm peak and (a)(ii) the corresponding UV-Vis spectrum and (c) Plot of ellipticity at 261 nm versus temperature of (**6**) with Li<sup>+</sup> (solid line) and added K<sup>+</sup> (dotted line) cations; Plot of fluorescent measurements (ATTO 550) versus temperature of (**6**) with Li<sup>+</sup> (solid squares) and added K<sup>+</sup> cations (25 mM) (open squares). Arrows indicate the direction of heating.

The oligomer (**6**) with Li<sup>+</sup> ions showed uniform particles (Fig. 7c and d) however, these were observed to aggregate after the addition of K<sup>+</sup> ions (Fig. 7e and f). Here, aggregation may be due to the K<sup>+</sup> ions inducing G-quartet stacking as well as shielding of the phosphate along the alkyl backbone of (**6**).

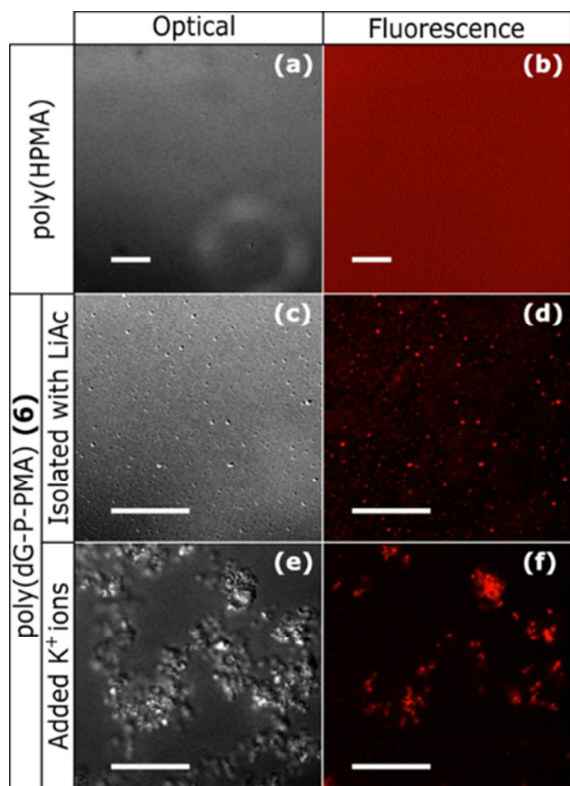


**Fig. 7** Optical and CLSM images of ATTO 550 stained (a and b) poly(HPMA), (c and d) Oligomer (**6**) isolated with lithium acetate and (e and f) Isolated oligomer (**6**) with added K<sup>+</sup> ions (25 mM) in water:isopropanol (10:1 v/v), respectively. Note the excitation laser output for poly(HPMA) has been amplified 10x. Scale bars are 20 μm.

## Conclusion

In summary, a nucleotide containing monomer has been synthesised by coupling HPMA to deoxyguanosine phosphoramidite. This monomer was then polymerised via RAFT producing an oligomer with low Đ and an M<sub>n</sub> indicative of hexamers. The deoxyguanosine-rich oligomer was then deprotected and detritylated and using circular dichroism shown to form anti-anti stacked G-quartet structures in the presence of cations. Analogous to DNA these structures melted, due to Hoogsteen bonding disruption. This work paves the way for the synthesis of nucleotide rich polymers with

improved degrees of polymerisation which show structural bonding analogous to G-quadruplexes observed in DNA.

## Conflicts of interest

There are no conflicts to declare.

## Acknowledgements

The authors acknowledge the assistance of Flinders Analytical-Flinders University in obtaining the ESI-MS. The authors wish to acknowledge funding support from Commonwealth Scientific and Industrial Research Organization (CSIRO) and an Australian Research Council Future Fellowship grant (FT130100211).

## Notes and references

- J. M. Berg, M. Jeremy, J. L. Tymoczko, L. Stryer and W. H. Freeman, *Biochemistry*, 2002, **6**, 654.
- S. Sivakova and S. L. Rowan, *Chem. Soc. Rev.*, 2002, **34**, 9-21.
- J. F. Lutz, A. F. Thünemann and R. Nehring, *J. Polym. Sci. Part A Polym. Chem.*, 2005, **43**, 4805-4818.
- H. L. Spijker, F. L. Van Delft and J. C. M. Van Best, *Macromolecules*, 2007, **40**, 12-18.
- Z. Hua, A. Pitto-Barry, Y. Kang, N. Kirby, T. R. Wilks and R. K. O'Reilly, *Polym. Chem.*, 2016, **7**, 4254-4268.
- R. McHale, J. P. Patterson, P. B. Zetterlund and R. K. O'Reilly, *Nat. Chem.*, 2012, **4**, 491-497.
- R. McHale and R. K. O'Reilly, *Macromolecules*, 2012, **45**, 7665-7675.
- P. K. Lo and H. F. Sleiman, *J. Am. Chem. Soc.*, 2009, **131**, 4182-4183.
- Y. Liu, R. Wang, L. Ding, R. Sha, N. C. Seeman and J. W. Canary, *Chem. Sci.*, 2012, **3**, 1930-1937.
- V. Kuryavii, K. N. Luu and D. J. Patel, *Nucleic Acids Res.*, 2007, **35**, 6517-6525.
- O. Stegle, L. Payet, J. L. Mergny, D. J. C. MacKay and J. L. Huppert, *Bioinformatics*, 2009, **25**, 374-382.
- A. I. Karsisiotis, N. M. Hessari, E. Novellino, G. P. Spada, A. Randazzo and M. Webba da Silva, *Angew. Chemie Int. Ed.*, 2011, **50**, 10645-10648.
- T. Ilc, P. Šket, J. Plavec, M. Webba da Silva, I. Drevenšek-Olenik and L. J. Spindler, *Phys. Chem. C*, 2013, **117**, 23208-23215.
- H. Han and L. H. Hurley, *Trends Pharmacol. Sci.*, 2000, **21**, 136-142.
- S. Neidle, *FEBS J.*, 2010, **277**, 1118-1125.
- S. Balasubramanian and S. Neidle, *Curr. Opin. Chem. Biol.*, 2009, **13**, 345-353.
- J. Bidzinska, G. Cimino-Reale, N. Zaffaroni and M. Folini, *Molecules*, 2013, **18**, 12368-12395.
- G. I. Livshits, A. Stern, D. Rotem, N. Borovok, G. Eidelshstein, A. Migliore, E. Penzo, S. J. Wind, R. Di Felice, S.S. Skourtis, J. C. Cuevas, L. Gurevich, A. B. Kotlyar and D. Porath, *Nat. Nanotechnol.*, 2014, **9**, 1040-1046.
- P. Tóthová, P. Krafčíková and V. Víglaský, *Biochemistry*, 2014, **53**, 7013-7027.
- ABI™ 3948 Nucleic Acid Synthesis and Purification System: Reference Manual, 2011
- S. Verma and F. Eckstein, *Annu. Rev. Biochem.*, 1998, **67**, 99-134.
- M. H. Caruthers, *Science* 1985, **230**, 281-285.

## Journal Name

## ARTICLE

- 23 C. Vargeese, J. Carter, J. Yegge, S. Krivjansky, A. Settle, E. Kropp, K. Peterson and W. Pieken, *Nucleic Acids Res.*, 1998, **26**, 1046-1050.
- 24 B. Li, Y. Du, T. Li and S. Dong, *Anal. Chim. Acta*, 2009, **651**, 234-240.
- 25 H. Vu and B. L. Hirschbein, *Tetrahedron Lett.*, 1991, **32**, 3005-3008.
- 26 C. Schuerch, *Annu. Rev. Phys. Chem.*, 1962, **13**, 195-220.
- 27 M. I. Elzagheid, E. Viazovkina and M. J. Damha, Synthesis of protected 2'-deoxy-2' fluoro- $\beta$ -D-arabinonucleosides. In *Current Protocols in Nucleic Acid Chemistry*. Edited by S. Beaucage. Vol. 1.7. 2002. p. Unit 1.7
- 28 P. Kujawa, H. Watanabe, F. Tanaka, and F. M. Winnik, *Eur. Phys. J. E*, 2005, **17**, 129-137.
- 29 I. Bischofberger and V. Trappe, *Sci. Rep.*, 2015, **5**, 15520.
- 30 U. Bhattacharjee, C. Beck, A. Winter, C. Wells and J. W. Petrich, *J. Phys. Chem. B*, 2014, **118**, 8471-8477.
- 31 H. Chen, S. S. Ahsan, M. B. Santiago-Berrios, H. D. Abruña and W. W. Webb, *J. Am. Chem. Soc.*, 2010, **132**, 7244-7245.
- 32 Y. Kang, A. Pitto-Barry, M. S. Rolph, Z. Hua, I. Hands-Portman, N. Kirby and R. K. O'Reilly, *Polym. Chem.*, 2016, **7**, 2836-2846.

Text: Propyl methacrylate oligomers with pendant guanosine monophosphate nucleotides can self-assemble in the presence of monovalent cations.

